Plastic ribbon THz waveguides

R. Mendis and D. Grischkowsky
School of Electrical and Computer Engineering and Center for Laser and Photonics Research, Oklahoma State University, Stillwater, Oklahoma 74078

(Received 5 June 2000; accepted for publication 19 July 2000)

We report an experimental and theoretical study of single mode, guided wave propagation in plastic ribbons. Using cylindrical THz optics, we obtain excellent quasioptic coupling between freely propagating THz waves and a single TM_0 waveguide mode. Dispersive, low-loss propagation is observed within the experimental bandwidth of 0.1–3.5 THz for 2-cm-wide, high-density polyethylene ribbon waveguides with dimensions of 150 μm thick by 10 mm long, and 120 μm thick by 20 mm long. Such ribbons show promise as a flexible THz interconnect with a controllable group velocity dispersion. © *2000 American Institute of Physics.* [S0021-8979(00)08720-X]

The continued improvements in device performance and the demand for ever increasing bandwidth will soon require the propagation of ps or subps pulses on micron or submicron sized wiring. This situation has forced the consideration of guided wave propagation effects for the interconnect between electronic chips and even down to the single chip level. Phenomena previously considered only by the microwave community in the frequency domain at GHz frequencies are now becoming manifest in the ps time domain at THz frequencies. An alternative to lithographically defined, high-bandwidth transmission lines on dielectric substrates is wave guided propagation of THz radiation, and the associated coupling between guided and freely propagating THz beams. Recently, efficient, broadband coupling of freely propagating THz pulses into circular and rectangular metal waveguides has been demonstrated,[1,2] and single-mode THz propagation in sapphire fibers has been reported.[3]

By configuring a dielectric waveguide into the form of a thin, wide ribbon, it becomes possible to utilize the fringing fields for technical and fundamental research applications. The planar geometry is amenable to photolithographic techniques, whereby active and passive devices, including coplanar transmission lines, can be fabricated onto the waveguide itself; these structures are then able to couple into and out of the waveguide. The feasibility of the THz ribbon waveguide as a transmission line and a circuit interconnect is enabled by the low loss factor,[4] flexibility, and ease of coupling into and out of the guide using either planar optics or cylindrical quasioptics. The waveguide propagation is also relatively stable to thickness variations of the order of $\lambda/10$.[5] In contrast to the previous work,[1–3] the group velocity dispersion (GVD) can be controlled by the thickness of the ribbon, making it possible to have a relatively broad frequency range for which GVD is negligible and within which THz pulses could propagate without distortion. It is also possible to obtain within other broad frequency ranges GVD values of the opposite sign to those of the metal and fiber waveguides,[1–3] thereby allowing for the subsequent pulse compression of the broadened pulses from these waveguides.

Here, we report an experimental study and theoretical explanation of single-mode propagation and quasioptic coupling of picosecond THz pulses in plastic ribbon waveguides. Dispersive, low-loss propagation is observed within the bandwidth from 0.1 to 3.5 THz for 2-cm-wide ribbon waveguides made of high-density polyethylene (HDPE), having nominal dimensions of 150 μm (thick) by 10.0 mm (long), and 120 μm (thick) by 20.0 mm (long). The large GVD of the waveguide causes extensive pulse reshaping and broadening, resulting in positively chirped output pulses. The experiment and calculations based on the well-known two-dimensional (2D) slab waveguide model[6] show that the linearly polarized (perpendicular to the plane of the ribbon) incoming THz beam couples predominantly only to the dominant TM_0 mode resulting in single-mode propagation, even though the wideband input spectrum extends beyond the cutoff frequencies of several higher-order modes.

The experimental setup is similar to that used to investigate THz propagation in metallic waveguides[1,2] and sapphire fibers.[3] Instead of the hyperhemispherical lenses used previously to couple the energy into and out of the guide,[1–3] the lens-waveguide-lens system employed here, inset of Fig. 1(b), uses plano-cylindrical lenses. The high-resistivity silicon cylindrical lens focuses the incoming THz beam only along one dimension producing an elliptic Gaussian beam for the amplitude, whose frequency-independent $1/e$ minor axis is only 100 μm. The unfocused $1/e$ major axis (8 mm at 1 THz) is inversely proportional to the frequency, and is oriented parallel to the ribbon. An identical optical arrangement is used at the exit face.

The reference pulse is obtained by removing the waveguide and moving the two silicon lenses to their confocal position. This pulse is shown in the inset of Figs. 1(a) and 2(a), and its amplitude spectrum in Figs. 1(b) and 2(b), shows a useful spectrum extending from 0.1 to about 3 THz. The measured propagated pulses through the 10- and 20-mm-long waveguides are shown in Figs. 1(a) and 2(a), respectively, and their corresponding amplitude spectra in Figs. 1(b) and 2(b). The incident 1 ps THz pulse has been stretched to about 20 ps with 12 major cycles of oscillation by passage through the short waveguide, and to about 40 ps with 29 major cycles of oscillation by passage through the long waveguide. The leading portions of these two output pulses exhibit a positive chirp, where high frequencies arrive later in time, opposite to what has been observed in the metal

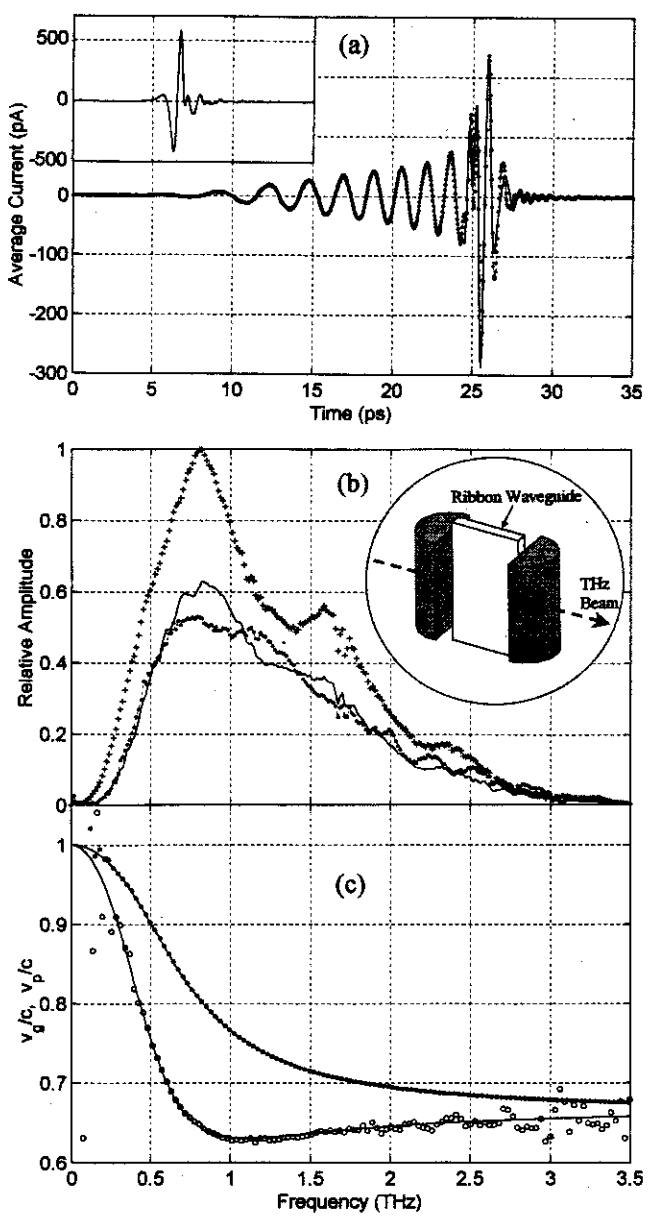

FIG. 1. (a) Measured (dots) and theoretical (solid line) propagated pulse through the short waveguide. The measured reference pulse is shown in the inset. (b) Amplitude spectra of the measured (dots) and calculated (solid line) propagated pulse, and measured reference pulse (crosses). The lens-waveguide-lens system is shown in the inset. (c) Upper curve gives the theoretical phase velocity v_p as a ratio to the free-space value c. The dots give the experimental values. Lower curve gives the theoretical group velocity v_g as a ratio to the free-space value c. The open circles give the experimental values.

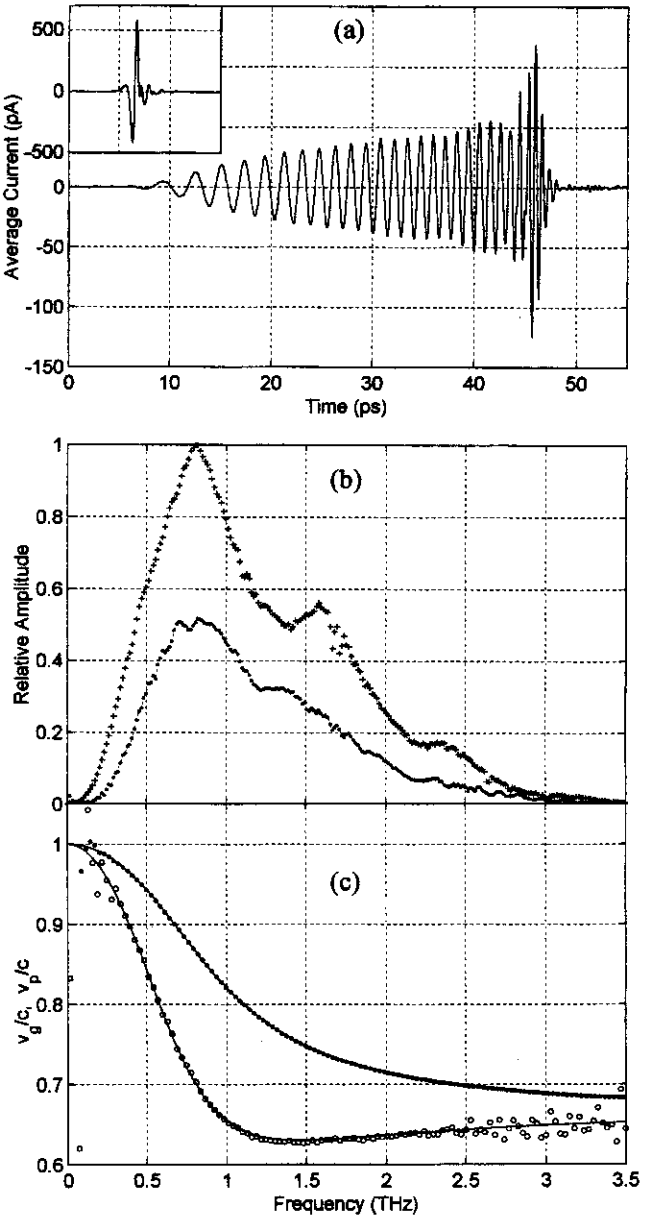

FIG. 2. (a) Measured propagated pulse through the long waveguide. The measured reference pulse is shown in the inset. (b) Amplitude spectra of the measured propagated pulse (dots), and measured reference pulse (crosses). (c) Upper curve gives the theoretical v_p/c ratio. The dots give the experimental values. Lower curve gives the theoretical v_g/c ratio. The open circles give the experimental values.

waveguides[1,2] and sapphire fibers.[3] The trailing portions of these output pulses exhibit slight interference effects at 25 ps, Figs. 1(a) and at 45 ps, Fig. 2(a).

The amplitude spectra of the propagated pulses, compared to the spectrum of the reference pulse, clearly exhibit very efficient wave-guiding characteristics. The loss in signal level is mainly attributable to coupling losses at the entrance and exit faces of the waveguide, since our measured power absorption constant of HDPE is quite low, less than 1 cm^{-1} throughout the available spectrum. It is also clear from the relatively smooth output spectra that there is no sharp low-frequency cutoff or any unusual oscillations (interference in the frequency domain due to multimode propagation) as observed in earlier investigations.[1,2] This smoothness in the amplitude spectra confirms single-mode propagation, with a cutoff frequency of zero.

The fundamental equation governing the input and output relationship of the system, assuming single-mode TM_0 propagation, can be written in the frequency domain as

$$E_{\text{out}}(\omega)=E_{\text{ref}}(\omega)TC^2\exp\{-j(\beta_z-\beta_0)z\}\exp\{-\alpha z/2\}, \tag{1}$$

where, $E_{\text{out}}(\omega)$ and $E_{\text{ref}}(\omega)$ are the complex spectral component at angular frequency ω of the output and reference electric fields, respectively; T is the total transmission coefficient

which takes into account the reflections at the entrance and exit faces; C is the coupling coefficient, the same for both the entrance and exit faces; β_z is the phase constant; $\beta_0 = 2\pi/\lambda_0$; α is the power absorption constant; and z is the distance of propagation.

The phase constant β_z was numerically evaluated using the nonlinear transcendental equation, characteristic of the slab waveguide.[6] β_z was experimentally determined using Eq. (1), and the measured relative phase obtained from the ratio of the complex spectra of the propagated and reference pulses, where TC^2 is real. The phase velocity (v_p) and group velocity (v_g) were then derived from β_z, and are plotted in Figs. 1(c) and 2(c) for the short and long waveguide, respectively. For this comparison, a thickness of 155 μm and a propagation length of 10.0 mm for the short waveguide, a thickness of 116 μm and a length of 20.1 mm for the long waveguide, were used as the fitting parameters, in good agreement with the measured values. Consistent with previous measurements,[7] a frequency-independent refractive index of 1.5 for HDPE was also used. It is seen that v_p and v_g approach that of bulk HDPE at high frequencies, while at very low frequencies they approach that of free-space c. This change over is due to the spatial power flow of the waveguide changing from containment within the core region at high frequencies, to a surface-guided wave traveling mainly in the free-space region at low frequencies. At the low frequency limit, v_g is very close to c, explaining the almost immediate arrival of the output pulses with respect to the arrival of the reference pulse, as shown in Figs. 1(a) and 2(a), with the same time synchronization. The maximum GVD is seen to occur in the low-frequency part of the spectrum, up to about 1 THz for the short and thick guide, Fig. 1(c), and up to about 1.4 THz for the long and thin guide, Fig. 2(c). This highly dispersive region, where v_g decrease as the frequency increases, produces the observed positive chirp in the time domain. An interesting feature in the v_g plot is the presence of a well-defined minimum region with zero GVD, which conveys the possibility of two different frequency components on either side of the minimum, propagating with the same v_g. This would cause an interference effect between these frequency components in the time domain, but will not be present in the amplitude spectra. The v_g curves were obtained from the numerical derivative of β_z and thereby have significantly more experimental noise than the v_p curves.

The quasioptic calculation of coupling and transmission coefficients assumes fundamental Gaussian beam propagation through the free-space paths. Coupling *from* and *to* the Gaussian beam is assumed to take place at planar phase fronts based on the confocal nature of the experimental system. Via the completeness and orthogonality of the waveguide modes,[2,6,8,9] the overall coupling (and reflection) loss, given by the product TC^2 in the frequency domain, can be expressed as

$$TC^2 = \frac{4\eta_p\eta_0}{(\eta_p+\eta_0)^2}\left[\int_A (\mathbf{E_i}\cdot\mathbf{E_p})dA\right]^2, \qquad (2)$$

where $\mathbf{E_i}$ and $\mathbf{E_p}$ represent the normalized electric fields of the fundamental Gaussian beam and the dominant waveguide mode, respectively, with their corresponding impedances η_0 and η_p, where η_0 is the impedance of free space. The overlap integral is calculated over the cross-sectional area of the guide, which includes the surrounding space.

The calculated absorption of a propagating mode of a dielectric waveguide[10] requires the absorption of the bulk material. We directly determined the absorption constant from the ratio (corrected for TC^2) of the amplitude spectrum of the propagated pulse of the long guide to the spectrum of the reference pulse, based on Eq. (1). The bulk power absorption obtained for HDPE was less than 1 cm^{-1} over our frequency range and was consistent with published data.[7] Our measured absorption was used on the short waveguide data to derive the theoretically propagated pulse. This comparison shown in Fig. 1(a) and the corresponding amplitude spectra in Fig. 1(b) clearly show excellent agreement between theory and experiment.

This study demonstrates the feasibility of the plastic ribbon waveguide as a low-loss, single-mode transmission channel for the THz region, capable of utilizing efficient quasioptic coupling. Ultralow-loss lines are possible by reducing the thickness of the ribbon such that most of the guided wave energy propagates outside the core region.[4] The performance can be further enhanced by the use of a very low-loss material such as high-resistivity silicon. Due to the ability to change the group velocity dispersion (GVD) by changing the thickness of the ribbon waveguide, large frequency regions with essentially no GVD can be obtained. In addition, by changing the sign of GVD of the ribbon waveguide with respect to that of the metal and fiber waveguides, mutual pulse compression should be possible, in analogy to dispersion compensation with optical fibers. The ribbon waveguides are particularly well adapted for THz time-domain spectroscopy (THz-TDS) studies of surface-specific molecular adsorption layers, or other thin films coating the waveguides due to the extensive fringing fields of the propagating THz waves.

This work was partially supported by the National Science Foundation and the U.S. Army Research Office.

[1] R. W. McGowan, G. Gallot, and D. Grischkowsky, Opt. Lett. **24**, 1431 (1999).
[2] G. Gallot, S. P. Jamison, R. W. McGowan, and D. Grischkowsky, J. Opt. Soc. Am. B **17**, 851 (2000).
[3] S. P. Jamison, R. W. McGowan, and D. Grischkowsky, Appl. Phys. Lett. **76**, 1987 (2000).
[4] C. Yeh, F. I. Shimabukuro, and J. Chu, Appl. Phys. Lett. **54**, 1183 (1989).
[5] J. E. Goell and R. D. Stanley, Proc. IEEE **58**, 1504 (1970).
[6] C. A. Balanis, *Advanced Engineering Electromagnetics* (Wiley, New York, 1989), pp. 414–441.
[7] J. R. Birch, Infrared Phys. **30**, 195 (1990).
[8] D. Marcuse, *Light Transmission Optics* (Van Nostrand Reinhold, New York, 1972), pp. 305–326.
[9] M. Bouda, Y. Nakano, and K. Tada, IEICE Trans. Electron. **E80-C**, 640 (1997).
[10] W. M. Elsasser, J. Appl. Phys. **20**, 1193 (1949).